

Paul W. Stackhouse Jr.<sup>1</sup>, Shashi K. Gupta<sup>2</sup>, Stephen J. Cox<sup>2</sup>, J. Colleen Mikovitz<sup>2</sup>, and Marc Chiacchio<sup>2</sup>

<sup>1</sup>Atmospheric Sciences Division, NASA Langley Research Center, Hampton, Virginia 23681-0001

<sup>2</sup>Analytical Services and Materials, Inc., Hampton, VA, 23666

## 1. INTRODUCTION

The Surface Radiation Budget (SRB) project at NASA, is a component of the Global Energy and Water Cycle Experiment (GEWEX), under the auspices of the World Climate Research Programme (WCRP). SRB estimates surface radiative flux quantities using satellite observations, re-analysis meteorology, and ozone measurements for input to parameterized radiation models. Release 2, currently being archived for distribution at the NASA Langley Atmospheric Sciences Data Center, improves the resolution to 1° latitude x 1° longitude, and upgrades many of the inputs and models.

This paper presents results from 5 years of processing. A comparison of the year-to-year variability is given for each of the 5 years. An assessment of the effect of the 1992 El Nino to the SRB relative to 1986 is made. The results are analyzed in terms of different time and space averages.

## 2. GEWEX SRB OVERVIEW

Production of the NASA/GEWEX SRB data set involves the processing of global atmospheric and surface data on a 3-hourly basis. These data are used in radiative transfer based algorithms to estimate the surface fluxes. Ultimately, the data set is aimed to support the validation of data assimilation and climate models, provide radiative boundary conditions for interdisciplinary studies, conduct research on the mean state and variability of the SRB, and applied to many industrial needs.

### 2.1 Input Data Sets

To compute surface fluxes at a 1° spatial and 3-hourly temporal resolution several types of the data sets are used. To obtain cloud information, the International Satellite Cloud Climatology Project (ISCCP) DX is used. The ISCCP "DX" pixel level data set contains radiance and cloud retrieval information from geosynchronous and polar orbiting satellites sampled to a nominal resolution of 30 km. All 30 km 'DX' pixels within a grid cell are averaged analogously to the methods of ISCCP (e.g., Rossow *et al.* 1996) to produce gridded radiance and cloud products that are required for the flux algorithms. To provide the necessary meteorological

*\*Corresponding author address:* Dr. Paul W. Stackhouse, Jr., NASA Langley Research Center, M.S. 420, Hampton, VA 23681; email: [p.w.stackhouse@larc.nasa.gov](mailto:p.w.stackhouse@larc.nasa.gov)

profile information including temperature and humidity, a global reanalysis is used. A reanalysis provides a better representation of the diurnal cycle of temperature and humidity relative to the Tiros Observational Vertical Sounder (TOVS) data that is mostly just at once per day. The Goddard Earth Observing System (GEOS) v.1 reanalysis provided by the Data Assimilation Office (DAO) of NASA's Goddard Space Flight Center is used to provide this information for this data release. In addition to the reanalysis, other new data inputs at higher resolution have been include. The most important of which is the 1.25° longitude x 1° latitude resolution column ozone from the measurements of the Total Ozone Mapping Spectrometer (TOMS). Other higher resolution data sets are being included such as high resolution surface type classification maps.

### 2.2 Flux Algorithms

The GEWEX SRB data products are computed using two shortwave (SW) and two longwave (LW) algorithms. For brevity only the results from two of the models are shown here. The shortwave data results from an upgraded version of Pinker and Laszlo (1992). This algorithm computes a broadband solar flux for each time stamp. The algorithm uses a two-stream delta-Eddington model to map broadband reflected fluxes at the Top-of-Atmosphere (TOA) to transmitted fluxes at the surface. The reflected fluxes at TOA are computed using narrow band to broadband relationships on the visible radiances and angular distribution models (ADMs) from the Earth Radiation Budget Experiment (ERBE). The model has been updated with new water vapor parameterizations and averaging schemes. A secondary algorithm is that described in Gupta *et al.*, (1999). This model is referred to as the Langley Parameterized Shortwave Algorithm (LPSA) since it employs several empirical and parametric relationships to account for various scattering and absorptive processes in the atmosphere. Results from the LPSA are available but not shown here.

In the longwave, the GEWEX LW Quality Check algorithm is a slightly upgraded version of Gupta *et al.* (1999). This algorithm uses broadband parameterizations of narrow band (10 cm<sup>-1</sup>) radiative transfer calculations as a function of water vapor and temperature to compute a clear-sky flux given the meteorological profile of the grid box. The model uses cloud fraction and the cloud top temperatures to prescribe the effects of clouds on the clear-sky flux using the same assumptions about cloud thickness mentioned above. TOA fluxes are currently not computed with this algorithm, but the model does allow

for nonblack surface emittances. A secondary GEWEX LW algorithm using the Fu *et al.* (1997) infrared radiative transfer model is also being tested. This radiative transfer model is nearly the same model used in the Surface and Atmospheric Radiative Budget (SARB) flux computations that are part of the Clouds and the Earth's Radiant Energy Systems (CERES) processing system. Results for the 5 years of LW fluxes are not yet available so we present the LW QC model fluxes here.

### 2.3 Processing Status and Currently

To date nearly 6 years of data have been processed for 3 of the 4 algorithms. The data are being archived at the NASA Langley Research Center Atmospheric Science Data Center (ASDC) for future public distribution. Portions of the data sets processed so far are available and can be obtained by contacting the author.

### 3. MONTHLY AVERAGED FLUX VALIDATION

Accompanying the processing of the SRB data is a concerted effort to validate the fluxes in time. Figure 1 shows a comparison of the flux estimates for the two algorithms used here versus measurements from the Baseline Surface Radiation Network (BSRN) for all sites and all months of 1993. We note that biases are  $-1.1$  and  $3.2$  for LW and SW respectively. The RMS errors (including bias) are  $17.5$  and  $21.3$   $W m^{-2}$  for LW and SW respectively. The RMS values represent an uncertainty estimate for the fluxes in any given grid cell.

### 4. INTERCOMPARISON OF 5 YEARS

For the study here, we examine the results from 5 years of SRB data: 1986, 1987, 1989, 1992, and 1993. During this time period there were two El Nino's. The first occurred in 1987 and the second in 1992. We first establish the year-to-year variability for each of the years to determine a baseline for distinguishing a discernable signal for El Nino effects on different spatial and temporal time scales.

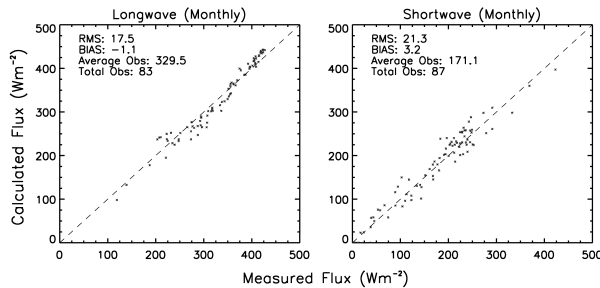


Figure 1: Monthly SW and LW flux comparisons between GEWEX SRB estimates and BSRN observations in 1993.

### 4.1 Global Annual Average

Table 1 presents the global annual averages for the various flux components for each of the 5 years. The averages compare well to the 4 year average of mid-seasonal months from Rossow and Zhang (1995) and to the Gupta *et al.* (1999) results. Note that the range of the variability in the non El Nino years is  $2 - 4$   $W m^{-2}$  for each component except for the Total Net flux which varies little between the 3 years. The 1987 El Nino falls within this range for each component. However, the 1992 El Nino establishes minima in the SW and Total Net components. The significance of this is not yet understood.

### 4.2 Zonal Annual Averages

The 5-year mean, minimum and maximum of the zonal annual average SW down, LW down, SW net and LW net fluxes are given in Figure 2. The shapes are consistent with our understanding the Earth's zonal surface radiation balance. The LW down fluxes are determined in large part by the temperature and moisture of the boundary layer which is maximum in the tropical areas. The SW downward fluxes are determined mainly by the planetary factors modified by the earth's major cloud patterns. The SW-net flux gives a net positive flow of energy to the surface while the LW-net gives a net negative flow of energy from the surface. Note that at the polar surface the SW-net roughly balances the LW-net. At TOA the LW-net dominates indicating the deficits of total net energy over the poles are due to atmospheric emission.

The SW quantities give the largest variation ranging up to  $\pm 6$   $W m^{-2}$  relative to the 5-year mean for zones near the poles. On average the range was about  $\pm 3$   $W m^{-2}$ . The LW differences showed a smaller range that was at most  $\pm 4$   $W m^{-2}$  and on average about  $\pm 2$   $W m^{-2}$ . The net SW and LW ranges were similar to the downward fluxes and the total was between the two. Given the level of variability the effect of El Nino does not appear to be separable from the noise on the zonal annual average scale.

Table 1: Global Annual averages for each of the 5 years processed and two previous SRB data sets.

	Zhang & Rossow (1995)	Gupta <i>et al.</i> (1999)	Non-El Nino Years			El Nino Years	
			SRB R2 1986	SRB R2 1989	SRB R2 1993	SRB R2 1987	SRB R2 1992
SW Down	193.4	184.7	186.7	186.7	189.2	187.2	185.8
SW Net	165.1	160.9	164.8	165.2	168.3	165.3	163.6
LW Down	348.3	347.8	347.5	344.5	343.6	347.1	346.1
LW Net	-45.8	-47.9	-44.8	-45.6	-48.1	-45.9	-45.8
Total Net	119.2	113.0	120.0	119.6	120.2	119.4	117.8

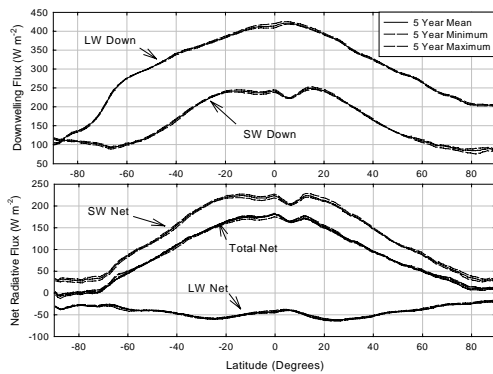


Figure 2: 5-year mean, minima, and maxima for the zonal annual averaged SW and LW downward fluxes (top panel) and SW-net, LW-net, and Total-net fluxes.

#### 4.3 Zonal January and July Averages

The zonal averages for the monthly means of January and July were also compared (not shown). There is a significant increase in variability at the month temporal average scale relative to the mean. The LW down flux variation was within  $\pm 6 \text{ W m}^{-2}$  relative to the mean for most of the globe. The SW variation was within  $\pm 10 \text{ W m}^{-2}$ . Larger variations were seen at the poles. So, fluctuations due to El Nino must exceed these ranges. In January, both the LW down flux for both the El Nino years exceeded the 5-year January mean in a region from  $3^\circ \text{ N}$  to  $5^\circ \text{ S}$  by greater up to  $6 \text{ W m}^{-2}$ . In the same region, the SW down fluxes were reduced relative to the 5-year January mean by up to  $8 \text{ W m}^{-2}$ . Outside of this region correlated fluctuations between the 1987 and 1992 El Nino's did not occur. Since these changes are correlated between the two years and consistent between LW and SW downward fluxes (thicker and lower clouds explain both differences), the differences found here may be indicative of the effect of El Nino, but more investigation is needed.

### 5. ASSESSING THE 1992 EL NINO

In this section we compare and contrast the SRB components between the year containing the 1992 El Nino event and 1986. The 1992 El Nino was relatively stronger than the 1987 El Nino. 1986 is representative of an average meteorological year without either an El Nino or La Nina events noted.

#### 5.1 Zonal Annual Averaged Differences

Figure 3 gives the zonal annual averaged difference of the net fluxes between 1992 and 1986. Most of variability associated with the difference is within the normal year-to-year variability. However, an interesting feature is an apparent shift from negative to positive in the SW-net flux from about  $10^\circ \text{ S}$  to  $15^\circ \text{ N}$  centered

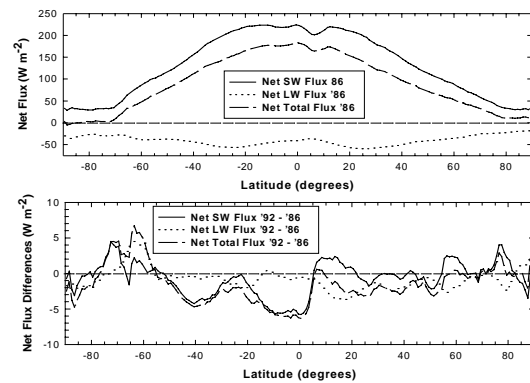


Figure 3: Zonal annual average of the SW-net, LW-net, and total-net fluxes for 1986 (top panel) and the difference between 1992 and 1986 (bottom panel).

about  $2^\circ \text{ N}$ . This is indicative of a southward shift in the cloudiness from N to S between the two years and is consistent with an El Nino caused event. More examination of this difference is needed.

#### 5.2 Global and Hemispheric Annual Cycle

Figure 4 gives the global and hemispheric annual cycles from the monthly averages of the net SW and LW fluxes. The interesting feature of note in this plot is the maximum in global averaged monthly differences obtained in the net SW for the month of March. The 1992 El Nino peaked at about this time. However, the peak differences in the LW-net are observed in the July time frame 4 months later. Further research is needed to determine if there is a cause and effect relationship between these two features.

#### 5.3 Regional Monthly Averaged Differences

The monthly averaged differences between 1992 and 1986 were computed for two different regions representing the tropical western (Box 1:  $20^\circ \text{ S} - 20^\circ \text{ N}$ ;  $120^\circ \text{ E} - 180^\circ$ ) and eastern (Box2:  $20^\circ \text{ S} - 20^\circ \text{ N}$ ;  $180^\circ - 120^\circ \text{ W}$ ) Pacific ocean. The cloud amounts and the corresponding SW and LW downward fluxes are shown in Figure 5 for the monthly average of the annual cycle in each region. The differences between these two years for each region is indicative of the shift of convective cloudiness from the western to the eastern Pacific. The cloud amounts decrease (increase) in the western (eastern) Pacific by 15% in January to March time frame between 1992 and 1986. Corresponding to this change the SW flux down increases by  $10 - 25 \text{ W m}^{-2}$  and the LW flux down decreases by  $10 - 17 \text{ W m}^{-2}$  in the western Pacific. By contrast the SW flux down in the eastern Pacific decreased from  $22 - 30 \text{ W m}^{-2}$  and the LW flux down increased about  $10 \text{ W m}^{-2}$ . This means that for the 1992 El Nino an east-west asymmetry occurred in the January to March time frame since the eastern Pacific region received  $20 \text{ W m}^{-2}$  less

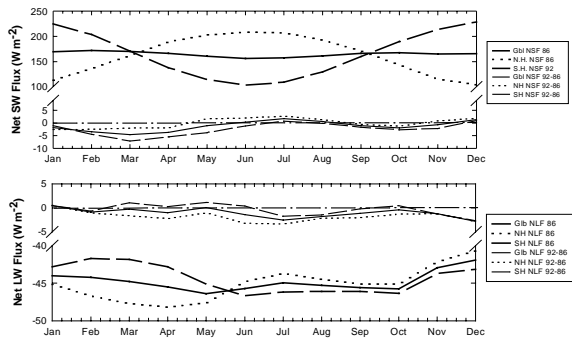


Figure 4: Each panel gives the global monthly averaged annual cycle for 1992 and the difference between 1992 and 1986 (scale break). The top panel gives the SW-net and the bottom gives the LW-net fluxes.

SW energy than the western Pacific gained in March. This asymmetry most likely explains why the zonal average differences between these two years showed equatorial differences. Also, interesting is the changes in SW and LW surface down fluxes nearly balanced in the western Pacific but the SW reduction dominates in the eastern Pacific. The LW fluxes between the two regions nearly cancel and explaining the lack of a LW effect in the zonal average.

## 6. CONCLUSIONS

The NASA/GEWEX SRB is in the midst of processing a 12 year data set which is on schedule for public distribution in the fall of 2002. Results from the 5 years of processing to date show general agreement with previous SRB data sets, but have differences that will be studied as the processing is completed. The interannual variability of the global annual average was found to be within  $\pm 2 \text{ W m}^{-2}$  with the least variability in the Total-net fluxes. Zonal annually averaged fluxes were found to vary  $\pm 2 \text{ W m}^{-2}$  and  $\pm 3 \text{ W m}^{-2}$  for the LW and SW respectively. Monthly average zonal fluxes showed interannual variability up to  $\pm 6 - 8 \text{ W m}^{-2}$ .

This paper also gave a basic assessment of effect of El Nino within the 5 years processed to date. Although the results here are preliminary, the effect of the 1992 El Nino was assessed on several different spatial and temporally averaged scales. Relative to 1986, there were small shifts in the SW and LW for zonal averages that could be attributed to asymmetric effects on the eastern and western Pacific regions that were up to  $20 \text{ W m}^{-2}$ . More analysis is needed to better quantify this El Nino within the context of a longer time series.

## ACKNOWLEDGEMENTS

Funding was provided under NASA grant MDAR-0506-0383 under the EOS Interdisciplinary Science program (NRA-99-OES-04).

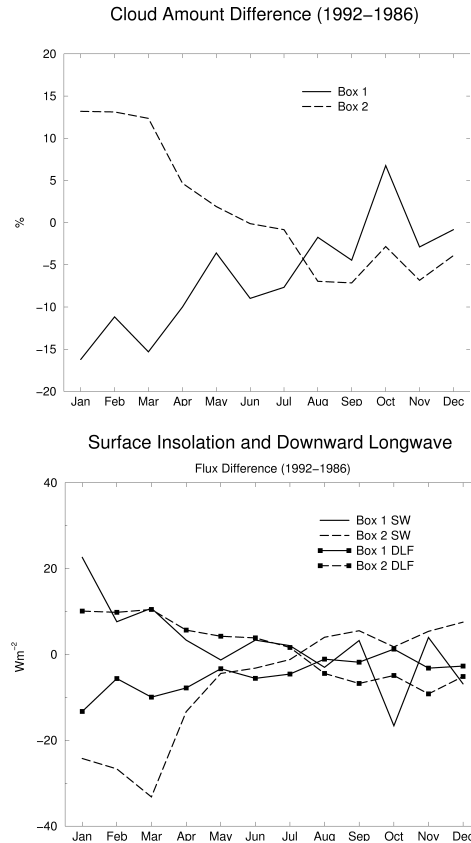


Figure 5: Regional average differences between 1992 and 1986 for cloud amount (top panel) and both SW and LW downward fluxes (bottom panel). Box one is the Tropical Western Pacific region ( $20^{\circ}\text{S} - 20^{\circ}\text{N}; 120^{\circ}\text{E} - 180^{\circ}$ ) and box 2 is the Tropical Eastern Pacific ( $20^{\circ}\text{S} - 20^{\circ}\text{N}; 180^{\circ} - 120^{\circ}\text{W}$ ).

## REFERENCES

- Fu, Q., K.-N. Liou, and A. Grossman, 1997: Multiple Scattering Parameterization in Thermal Infrared Radiative Transfer. *J. Atmos. Sci.*, **54**, 2799.
- Gupta, S. K., N. A. Ritchey, A. C. Wilber, C. H. Whitlock, G. G. Gibson, and P. W. Stackhouse Jr.: 1999: A Climatology of Surface Radiation Budget Derived From Satellite Data. *J. Climate*, **12**, 2691-2710.
- Pinker, R. and I. Laszlo, 1992: Modeling of surface solar radiation: Model formulation and validation. *J. Climate Appl. Meteor.*, **24**, 389-401.
- Rossow, W.B., A.W. Walker, D.E. Beusichel and M.D. Roiter, 1996: International Satellite Cloud Climatology Project (ISCCP): Documentation of New Cloud Datasets. WMO/TD 737, World Meteorological Organization, Geneva, Switzerland, 115 pp.
- Rossow, W.B., and Zhang, 1995: Calculation of surface and top of atmosphere radiative fluxes from physical quantities based on ISCCP data sets, 2, Validation and first results. *J. Geo. Res.*, **100**, 1167 - 1198.